Journal of Cancer Research and Clinical Oncology
https://doi.org/10.1007/s00432-023-04815-x

RESEARCH

Classification of skin cancer stages using a AHP fuzzy technique within the context of big data healthcare

Moslem Samiei[1] · Alireza Hassani[2] · Sliva Sarspy[3] · Iraj Elyasi Komari[4] · Mohammad Trik[5] · Foad Hassanpour[6]

Received: 24 March 2023 / Accepted: 23 April 2023

Abstract

Background and objectives Skin conditions in humans can be challenging to diagnose. Skin cancer manifests itself without warning. In the future, these illnesses, which have been an issue for many, will be identified and treated. With the rapid expansion of big data healthcare framework summarization and precise prediction in early stage skin cancer diagnosis, the fuzzy AHP technique produces the best results in both of these fields. Big data is a potent technology that enhances the standard of research and generates better results more rapidly. This essay gives a way to group the stages of skin cancer treatment based on this information. The combination of support vector machine multi-class classification and fuzzy selector with radial basis function-based binary migration classification of virtual machines is put through a number of experiments. The connections have been categorized.

Analysis method These examinations have determined whether the tumors are malignant or benign and how malignant they are. The images of spots on the skin acquired from laboratory images make up the data set used for processing. We have talked about how to handle and process large datasets in the area of classification using MATLAB, like skin spot images.

Findings Our technique outperforms competing approaches by maintaining stability even as the size of the data set grows rapidly and with little error. In comparison to other methods, the suggested approach meets the accuracy criterion for correct classifications with a score of 90.86%. As a result, the proposed solution is viewed as a potentially useful tool for identifying mass stages and categorizing skin cancer severity.

Keywords Big data · Health care · Skin cancer · Fuzzy AHP technique

Introduction

One of the most difficult parts of cancer treatment today is cancer diagnosis. The prognosis of cancer patients relies on an early cancer diagnosis. (either in the primary stage or in the second stage). When cancer is discovered in the third or later phases, it becomes more difficult for the patient to survive. The fatality rate of this malignancy can be reduced with early identification. However, using mammography scans to manually diagnose this cancer is a difficult task that always calls for a specialist (Jabeen et al. 2023).

If the data can be managed and analyzed by tools to solve many issues, such as identifying patterns that lead to cancer diagnosis, then single patient records frequently produce enormous amounts of data. Numerous mutations and combos that occur in tumor cells have been thoroughly researched (Manogaran et al. 2018; Kunkel et al. 2021; Vahidi Farashah et al. 2021a, b). Researchers select large data sets and spot changes to research specific tumors The

✉ Mohammad Trik
trik.mohammad@gmail.com

1 Department of Industrial Engineering, Islamic Azad University, Zahedan Branch, Zahedan, Iran

2 Center for Physics Technologies: Acoustics, Materials and Astrophysics, Department of Applied Physics, Universitat Politècnica de València, València, Spain

3 Department of Computer Science, College of Science, Cihan University-Erbil, Erbil, Iraq

4 Department of Computer Engineering, Andimeshk Branch, Islamic Azad University, Andimeshk, Iran

5 Department of Computer Engineering, Boukan Branch, Islamic Azad University, Boukan, Iran

6 Faculty of Information Technology and Computer Engineering, Azarbaijan Shahid Madani University, Tabriz, Iran

Published online: 02 May 2023

tools used by healthcare professionals to identify cancer are efficient. Bowel changes, chronic back pain, an unusual cough, rectal bleeding, urinary changes, and blood in the pee are all signs of early cancer (Speckemeier et al. 2022; Madani et al. 2021). The majority of cancers start as cutaneous tumors, and they most frequently affect the glands, breasts, testicles, and glands or lymph nodes. A small number of abnormal cells can be found using this kind of test, which is used to identify cancer. People can now develop a variety of cancers, including stomach cancer, brain cancer, breast cancer, pancreas cancer, and other excruciating cancers. Current procedures for gathering and processing crucial data about cancer patients demand a lot of work and computations (Trik et al. 2022; Radhoush et al. 2018; Rezaee et al. 2021). The availability of accurate information in real time is typically prevented by these processes' significant delays and proneness to errors. the use of the cloud as a novel technology; Electronic delivery of medical services has benefited significantly from the internet infrastructure and novel solutions. In reality, the emergence of the cloud computing phenomenon has led to a fundamental shift in how new, developed, scaled-back, and updated information technology services are provided (Trik et al. 2021a, b; Ghobaei-arani and Mahdi Babaei 2021). Because it is inefficient to manually review dermoscopic images, researchers in the field of computer vision used a number of algorithms to categorize the skin lesion. Some disadvantages of the current automated systems are their poor accuracy and lengthy computation times (Khan et al. 2023).

The medical treatment of damaged skin cells in a staged manner forces the predetermination of skin cancer phases (Hosseini 2022a, b; Ha et al. 2019). In the field of medicine, we are able to retrieve images of damaged components and identify the stages early. Medical data, however, can be organized, semi-structured, or unstructured. A summary of the unstructured data that forms the basis of predictive analytics is given by Sun et al. (2022), Chenarlogh et al. (2019). Here is some information on the use of unorganized data in predictive analytics and its potential. The goal of the resource management system in the classification of data for health care is to ensure that the criteria for the classification of the severity of cancer diagnosis are met. Additionally, the resource management mechanism should assess each resource's current condition in the health care environment to provide algorithms for better physical resource allocation or virtual resource allocation, which will lower operating costs in this environment (Darbandi et al. 2020; Rezaeipanah et al. 2021). Load balancing is necessary in big data processing for effective management of data classification. Requests will be dynamically and equally distributed among all data with effective load balancing, guaranteeing the equitable and effective distribution of each class of data. The stratification of skin cancer is diagnosed with greater accuracy thanks to this process, which also maximizes the use of available resources. Finding a suitable mapping for the classification of big data for cancer care is the goal of load balancing. The goal of this study is to use big data to apply the classification of cancer stages and healthcare services in accordance with the severity of skin cancer. We use the ARIMA model for the data of this research, which is the big data related to the pharmaceutical consumption related to different states of America in the years 2018–2021. We predict and estimate the required resources, and we tried to use the proposed algorithm, which has the lowest percentage of error in the forecast and is very close to the reality of the resources of a request. Then, we use the fuzzy AHP algorithm to supply the resources of each request according to the possibilities of local and non-local resources. This algorithm is based on the profit and profit parameters. Vari selects the most suitable resource and assigns it to the request, then the proposed methods are implemented and the results are compared with the other two methods. In short, our contribution to this article is as follows:

- Using the ARIMA model to accurately classify skin cancer care.
- Application of the fuzzy AHP technique to accelerate big data processing in health care for skin cancer diagnosis.
- Reduce response time.

The rest of this paper is organized as follows: Section "Related Work" contains the background. Fuzzy AHP techniques to determine the optimal cloud and resource forecasting technique using the ARIMA algorithm are presented in Section “Proposed method”. Section “Evaluation” shows the proposed model's evaluation and simulation, and the results and future work are discussed in Sections 5 and 6.

Related work

One of the most prevalent issues in the field is skin cancer. Treatment is likely to lessen this once it has been identified. The most dangerous form of skin disease is melanoma. It can be addressed, though, if caught early enough (Jeon et al. 2023). However, if this form of cancer is discovered too late, it may be dangerous. The cells that give the skin its color give birth to the tumor known as melanoma. Under the impact of UV rays, these cells, called melanocytes, produce a pigment called melanin (Manogaran et al. 2018; Dlamini et al. 2020). The use of a new technique for categorizing multi-class skin lesions that combines deep learning characteristics and an extreme learning machine is suggested (Afza et al. 2022). The five main steps of the suggested strategy are picture assimilation and contrast amplification. employing transfer learning for deep learning feature extraction. A

hybrid whale optimization technique and entropy mutual information are used to choose the best features. (EMI). a collection of chosen attributes put together using a modified canonical correlation-based method. Extreme machine learning-based classification is the last step. The feature selection process increases the system's accuracy and computational effectiveness. HAM10000 and ISIC2018, two publicly accessible datasets, were used in the experiment. The obtained accuracy in the two datasets is 93.40 and 94.36%. They are prevalent in the military or mole. Numerous variables, including ultraviolet radiation, mechanical harm, thermal or chemical burns, etc., can cause melanocytes to degenerate. Melanoma spreads rapidly and targets other organs, making it more dangerous than other forms of skin cancer. vascular system (Pethuraj et al. 2023; Mozaffari and Houmansadr 2020). Melanoma is a severe condition, but it can be treated if found early. So pay close attention to the skin, particularly the mole. In Khan et al.'s (2021a, b) study, mobile health units that function as nodes capture skin data using specialized technology. The cloud is used to process collected samples using a novel multimodal information fusion framework that first segments skin lesions before classifying them. The results are outstanding when compared to the prior situation, and five benchmark skin datasets (ISBI 2016, ISIC 2017, ISBI 2018, ISIC 2019, and HAM 1000) are utilized to evaluate segmentation and classification frameworks using average accuracy, false negative rate, sensitivity, and computing time. Everyone is not equally at risk of developing melanoma. But make sure to see your dermatologist frequently if any of the following pertain to you (Ha et al. 2022; Jung et al. 2021; Rafiee and Mirjalily. 2020). The Min–Max normalization approach was used by Gordon et al. (2016) and Trik et al. (2021a, b), to classify the stages of cancer using radionics. Ajmal et al. (2022) present an architecture based on the fuzzy entropy slime mold method and deep learning for the multi-class categorization of skin lesions. They initially enhanced the training data using the data augmentation technique, which they then utilized to train two fine-tuned deep learning models, such as Inception-ResNetV2 and NasNet Mobile. Then, in the following phase, they trained both models using transfer learning on the boosted dataset and got two feature vectors from the newly tweaked models. The experimental procedure produced accuracy of 97.1% and 90.2% better than existing strategies when applied to two datasets, including HAM10000 and ISIC 2018. The accuracy is increased by integrating the classification with the random forest method. This initiative also includes a multi-technology standard for categorizing stages as malignant or benign. Structured co-occurrence matrix (DGV), which organizes the classification method for classification as malignant and benign, is the main focus of Speckemeier et al. (2022). Additionally, it uses the DGVM method to extract the features from node images. DGV is coupled with Laplace, Gaussian, and Sobel filters for improved classification, which divides them into malignant or benign spots as well as malignant levels. This approach demonstrates that the SVM classifier performs better classification than the decision-based ANNs, MLPs, and classifiers from the overview of all concepts. In comparison to using individual classifiers, combining with classifier technology produces more accurate outcomes. For multi-class skin cancer classification, a two-stream deep neural network information fusion architecture is presented. The suggested approach consists of two streams: first, a fusion-based contrast enhancement methodology is suggested, which feeds enhanced images to a DenseNet201 architecture that has already been trained. A skew-controlled flame-thrower optimization approach is then used to optimize the extracted features. In the second flow, the pre-trained MobileNetV2 network's deep features are extracted and sampled using the suggested feature selection framework. The simulations are run without any data augmentation steps and achieve accuracy of 96.5%, 98%, and 89% (Attique Khan et al. 2022). It was discovered, as a result of a study by Gorry (2020) that suggests the concept of machine learning techniques, that SVM and some machine learning techniques are helpful for skin cancer classification with a reliable result. In comparison to using individual classifiers, combining with classifier technology produces more accurate outcomes. Additionally, the author assesses the primary skin cancer prediction methods that have been put forth to date and identifies some of their respective advantages and disadvantages. Deep learning techniques were used to study non-cellular skin cancer by Janda et al. (2019) and Forouzandeh et al. (2018). by Ulrich et al. (2016) used a web application to demonstrate how deep learning apps can be used to diagnose skin cancer. To identify skin cancer subtypes in histopathology slides, Abedini et al. (2019) created a deep neural network. They discovered that it performed just as well with three pathologists. Berahmand et al. (2022) and Rezaeipanah et al. (2020), confirmed pathological response on a dataset that included NELC treated with chemotherapy and surgery by fusing CNNs models with RNeN and using seed point tumor localization. As radiomics enhances findings from these kinds of images, Forouzandeh et al. (2015) compared delta radiomic features with non-delta features extracted from clinical tomographic images.This paper also employs conventional radiomics features to enhance efficiency. Khan et al. (2021a, b), classified the skin lesion image samples they had received from various servers.. The two modules of their approach are localization/segmentation and classification of skin lesions. They suggest a hybrid approach for the localization module that combines binary pictures produced by a 16-layer convolutional neural network model with salient segmentation based on the high-dimensional contrast transform (HDCT). Using Bayesian networks,

Andrew et al. (2021) enhanced the local tumor and tumor response before and after radiotherapy. Local control prediction is enhanced by combining with the created Markov blanket technique and envelope-based approach. As previously discussed in radiomic-based prediction, Kim et al. (2021) suggested a skin cancer radiomic-based prediction model. To address some limitations of the radiomic approach, this radiomic-based algorithm is combined with belief function modification and sparse learning (Yoosefdoost et al. 2022; Sheikhpour et al. 2023). They choose some features based on subsets of predictive features for further processing, in contrast to Shao and Feng's (2022) emphasis on skin cancer prediction using a large number of high-dimensional datasets. To forecast local control data sets of cancer patients after radiotherapy, Zia and Bukhari (2022),suggested neural networks. Their aggregated model performs better than the completely connected multilayer design. Guy et al. (2015) use a map-reduce architecture to demonstrate the effectiveness of parallel SVM while predicting and researching skin cancer. There has been a substantial amount of study dedicated to enhancing feature selection's effectiveness. For feature selection (Vafaeinik et al. 2022; Dindar et al. 2022; Trik et al. 2022), presented a collaborative GA algorithm with a configurable size. This algorithm employs the approach of "divide and rule" within the context of communal coevolution. A binary genetic algorithm (GA) basedfeature selection strategy was proposed by Zhang et al. (2022). This algorithm proposes a standard combination to strike a balance between local exploitation and global algorithm discovery, and it does so by employing a boosted memory technique to update local particle representatives without degrading prominent genes in particles. The GA algorithm's velocity update equation is tweaked in accordance with Newton's second law of motion, as proposed by Cao et al. (2022). For massively parallel optimization of high-dimensional problems, Zhang et al. (2020) provide a GA-based feature selection strategy. Using minimal GA and MI, Wang et al. (2020) created a feature selection system. To identify and remove non-cotton fibers, Tang et al. (2023) presented a two-stage feature selection strategy that combines an IG filter with a binary PSO overlay (PSO). Using Bi-Normal Separation (BNS) or IG as the first stage and Markov Blanket Filter (MBF) as the second, suggested a two-step feature selection approach for text categorization. Using a filter-based method (the RReliefF algorithm) and a multi-objective binary GWO with cuckoo search, Lei et al. (2022) suggested a two-stage feature selection approach for financial forecasting modeling. For the purpose of fault identification in complicated mechanical systems, Cheng et al. (2023a, b) suggested a two-stage feature selection approach using ReliefF and PSO. To improve model prediction, Cheng et al. (2023a, b) suggested a two-stage feature selection approach based on the orthogonal greedy algorithm. (OGA). Using C-Sq, a divergence from the Poisson distribution, a discrimination-based feature selection (DBFeature Selection), and a relative recognition criterion based on feature selection, developed a two-stage feature selection technique for text classification. In the second stage, he proposed using GA. The suggested method is compared to other two-stage feature selection methods in Table 1.

Table 1 Comparison of the proposed method with other existing methods

References	Objectives	Optimization methods		Area
		Stage 1	Stage 2	
Janda et al. (2019)	Accuracy	SGA	NSGA	Fault diagnosis for complicated
Jeon et al. (2023)	Diagnostic rate	Integrating of IG, DP, ReliefF, and GR	Improved GA	Modeling of financial forecasting
Andrew et al. (2021)	Error rate, number of features	C-Sq,, BD, RDC	SGA	Classification of gene expression data
Ulrich et al. (2016)	Accuracy	CSQ	Regression model with PSO	Classification of text
Speckemeier et al. (2022)	Diagnostic rate, Error rate	BD, GR	PSO	Classification of text
Abedini et al. (2019)	Accuracy	Integrating of DP, IG, ReliefF, and GR	MBF	Online detection system of foreign
Dhiman et al. (2022)	Error rate	GR	Regression model with BPSO	Model forecasting
Dlamin al. (2022)	Accuracy	C-Sq, DP,, RDC	GA	Prediction of bankruptcy
This work	Accuracy, number of features	SVM	Combination of multi-class classification of support vector machine and fuzzy selector	Classification of high-dimensional data

Proposed method

This section proposes an approach based on the AHP fuzzy technique to determine the optimal cloud and a resource prediction technique using the ARIMA algorithm. Also, to make a balance during the tasks' processing, the fuzzy selector-based VM migration technique was used to move a VM from a server with a high load to a server with a low gear. The structure of the proposed architecture is composed of two local and global parts. The local function should be checked first to deliver a request to the international part; if the local domain does not satisfy the conditions, the request is given to the worldwide part. Since the proposed method has a hierarchy architecture, the user request is given to the local data part. It is analyzed and monitored by the local analyzer to predict the resources. On this basis, the list of paid requests is first created, and then the extent of available resources is estimated by the ARIMA algorithm. The structure of the proposed architecture is so that it is assumed each CDC has a Broker. The Broker related to each CDC first receives and analyzes the requests of the users referring to this CDC. If the number of resources to execute the requests of the users is available, execute them and return the results to the users of that CDC. Still, suppose the Broker cannot execute the users' requests using the available CDC resources. In that case, it should choose the appropriate CDC from the associated CDC, using the AHP fuzzy algorithm, which every Broker access (Look at Fig. 1). As a result, for every CDC, there is a Broker wherein there are the following components:

- Request Monitoring is responsible for monitoring the number of users' requests, and Resource Monitoring is responsible for monitoring the number and the capacity of the resources available in a CDC.
- Resource Estimator is responsible for estimating the resources required for user requests using the ARIMA prediction algorithm, a time-dependent value prediction method.
- CDC Selector is responsible for selecting a CDC using the AHP fuzzy algorithm if a Broker is not able to execute the local requests using the resources of that CDC.

The structure of the Broker, along with its components, is shown in Fig. 1a, b.

Also, after choosing the server to process, a fuzzy selector-based VM migration technique so that if it becomes congested during processing and due to hardware or software violations, its VM can be migrated to a low-load or available idle server, and therefore the congestion and increase in runtime in the servers are prevented.

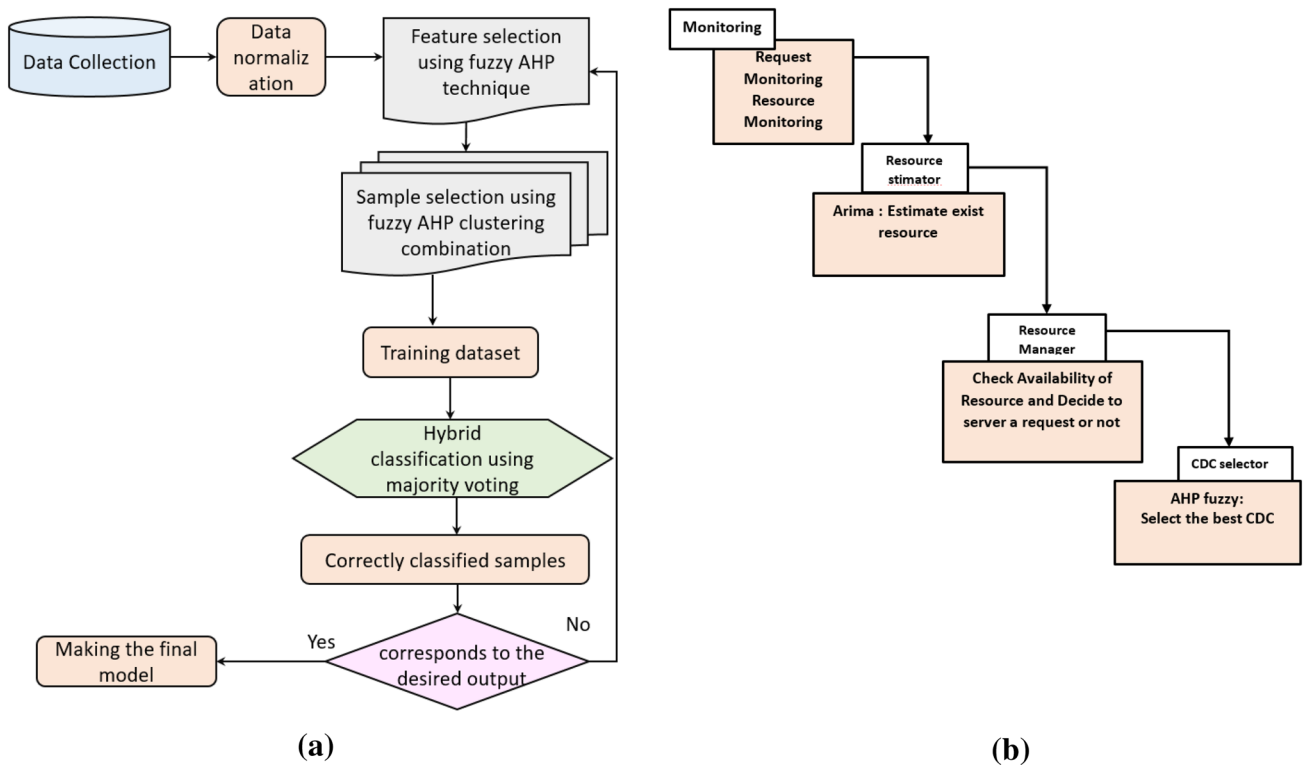

Fig. 1 Flowchart of classification steps for the proposed solution and Broker structure with its components

Problem formulation

In this part, the variables and formulas used in the proposed method are investigated. The user variable represents the users who are shown as an array in the form of user = {$u1, u2,\ldots,un$}.The allowed limit for responding the jth request of the ith user indicated by Req_j^i. The high supply threshold, the number of requests of each user, the number of requested resources, and the number of available resources are denoted by Threshold, Req-count, Res-req, and Resource, respectively. The users' request puts in the Q-req queue to be responded to. In this method, the CDC has been used, and their numbers are shown by N-CDC. It is possible that the local CDCs, i.e., LCC, can not meet the needs and a confederation is required, where the GCC are used. The service time threshold denotes by tts. For each CDC, some hosts are considered which are shown as $\text{Host}_j\text{-cdc}_i$. Each host of the set of VMs defined as VMi-hostj. The quality of service (QOS) measured according to the profit (b) and the cost (C_k). In addition, the distance between these CDCs ($D_{i,j}$) and the availability of the same type of VM (STVM) and a set of cloud providers. Table 2 introduces the main notions of the variables used in our structure. In this section, the variables and formulas used in the proposed method are examined.

Table 2 Notations and abbreviation signs

Req_j^i	Request j of user i
$\text{Host}_j\text{-cdc}_i$	The host of each cdc
C_k	Cost
RO	Random optimization
Stvm	Availability of the same type of virtual machine
LR	Likelihood ratio
Tts	Response time threshold
X_n	Input parameters
Y_n	Output parameters
y^i	The extent of local resource services
G^i	The amount of public resource services
HR	Hazard ratio
WL	Workload
μ	Average workloads
$CSCS$	Classification of Skin Cancer Stages
$\theta[j]$	Moving average model parameters by workload type
$\mathcal{E}$	White noise
$AR[i]$	Autocorrelation prediction model
$\phi[j]$	Autocorrelated prediction model parameters
L	Delay
CI	Confidence interval
$D_{i,j}$	Distance between cdcs
AUC	Area under the curve

Theoretical analysis

In most cases, this model is shown as ARIMA(p,d,q), where p, d, and q are non-negative real numbers that determine the degree of autocorrelation, integration and moving average. ARIMA models form an important part of the Box-Jenkins approach to time series models. If one of the components is equal to zero, it is usually written as AR, I, or MA. In the time series, there is an operator called LAG or delay, through which the previous workload can be calculated from the current workload according to the Eq. (1).

$$l \cdot w_t = w_{t-1}. \tag{1}$$

The value of L in the Eq. (2) represents the LAG operator. This prediction model is also a combination of the previous two models. with the difference that it uses the LAG operator to reach the next workload.

$$\left(1 - \sum_{i=1}^{p} \varphi_i L^i\right)(1-L)^d y_t = \left(1 + \sum_{i=1}^{q} \theta_i L^i\right) e_t. \tag{2}$$

In the above relationship, d is the root of the $1 - \sum_{i=1}^{p} \varphi_i l^i$ polynomial. $\theta_1 \ldots \theta_q$ are the parameters of the MA prediction model, which are determined according to the type of workload. ε_t is a random amount of white noise.

$\phi_{1\ldots}\phi_p$ are the parameters of AR prediction model which are determined according to the type of workload. Set the mean $E(X_t) = \mu$; of the generic time series $\{X_t, t = 1, 2,\ldots,n\}$ to be; the ARIMA(p, d, q) model may be written as (3).

$$\varphi(B)\left(\nabla^d X_t - \mu\right) = \theta(b)\varepsilon_t, \quad t > d, \tag{3}$$

where $B, BX_t = X_{t-1}$, gives the d- order differential operator and ∇^d, $\nabla^d X_t = (1-B)^d X_t$ stands for the backward shift operator.

Additionally, the definitions of the backward shift operator polynomials $\varphi(B)$ and $\theta(B)$ are

$$\begin{aligned} \varphi(B) &= \left(1 - \varphi 1^B - \varphi 2^{B^2} - \cdots - \varphi p^{B^p}\right., \\ \theta(B) &= \left(1 - \theta 1^B - \theta 2^{B^2} - \cdots - \theta q^{B^{pq}}\right., \end{aligned} \tag{4}$$

Receiving the requests

In algorithm No. 1, the requests are first placed the request queue and, based on the need, are referred to the desired resource. This algorithm shows how the requests are placed in the queue. Since each user has a variety of requests, every user request is placed in the queue (lines 2–4). This process is iterated for all users (line 1). In the following, it is defined what resource is required for each request (lines 6–8).

Algorithm 1: add Request to Queue

1: $for\ i\ \leftarrow 1\ to\ n\ do$
2: $for\ j\ \leftarrow 1\ to\ Req\_Count_j\ do$
3: $ADD\ Req_j^i\ to\ Request\_queue$
4: $end\ for$
5: $While(Request\_queue\ is\ not\ empty)$
6: $foreach\ req\ in\ Request\_queue\ do$
7: $Send\ req\ to\ LCC$
8: $end\ for$

Monitoring phase

This phase is responsible for collecting the received requests and the available and existing resources. The monitor phase includes two request and resource phases. The resource monitoring phase is responsible for gathering information on the productivity of resources, the capacity of resources used and checking the maximum number of VMs. The request monitoring phase is responsible for gathering information about the workload of the requests sent by the users. This monitored information is collected and integrated by these two subcomponents and is stored to be used by the other phases in the knowledge base.

Algorithm No. 2 is used to monitor the services of each resource in LCC (local resource) or GCC (global resource). Until there are free resources (line 1), the algorithm is executed. The algorithm starts with a while loop that continues as long as the resource is available (i.e., not equal to zero). Within the while loop, there are two nested for loops (one for *i* and one for *j*), which iterate over all possible combinations of *i* and *j* within the limits of *n* and *m*. If the cdc is available in the lcc (line 4), the algorithm calculates y^i using the available cdc and the coefficients x_1 to x_j. This algorithm checked both global and local resources, The result is assigned to y^i. If the cdc is not available in the lcc but is available in the gcc (line 7), the algorithm enters another nested for loop to calculate G^i using the available cdc and the coefficients x_1 to x_j. The result is assigned to G^i. If the cdc is not available in either location (line 11), the algorithm sets the resource variable to 0, which will cause the while loop to terminate and the algorithm to exit. It's difficult to say for sure without more context, but it seems likely that the calculations being performed using the cdc and coefficients are part of a larger process involving resource allocation or optimization. but the main priority is monitoring local resources. First, the amount of local resources' services is checked; if there are no local resources, it has referred to the local resources located in the general cloud federation, and for each of the available CDCs in the GCC, the services are checked (lines 8–12).

Algorithm 2: Resource monitoring

*1: while (*resource*! =0) {*
2: $for\ i \leftarrow 1\ to\ n\ do$
3: $for\ j \leftarrow 1\ to\ m\ do$
4: if (cdc is available in our lcc)
5: $y^i = x_1 cdc_i + \cdots + x_j cdc_i$
6: $else$
7 : if (cdc is available in gcc)
8: $for\ i\ \leftarrow 1\ to\ n\ do$
9: $for\ \ j \leftarrow 1\ to\ m\ do$
10: $G^i = x_1 cdc_i + \cdots + x_j cdc_i$
11: $else$
12: do resource = 0

}

Prediction phase

The prediction phase of the resource is responsible for estimating the number of available resources for servicing the requests. If the allocated resources are not able to fully satisfy the demands, the low supply occurs, and if the allocated resources exceed the real requirements, high supply occurs. Therefore, an accurate estimation of recognizing the resource request needs can be obtained using the ARIMA algorithm. In algorithm No.3, a semi-code of ARIMA has been shown, which is used to predict the resources needed for every request. First, every user request has been considered as an input, and a set of features of each request is defined using the x, each of these features will be effective in allocating the resource. The amount of resources needed for each request is calculated according to the features of each request and the tracking factor of every change (line 4). The maximum real request is calculated by Z.

Resource management phase

After measuring the resource for a specific request, the resource predictor sends the source of this request to the resource manager. The resource manager checks the availability of the resources and decides on the serviceability of the new request. If there is no available resource for the CDC host, it is tried to find an optimal unified CDC using AHP. If the resource is available, its size should not be much more than the resources needed for the request so that the high allocation is prevented.

Algorithm 3: Arima Prediction

```
While (req >0) {
For i ← 1 to 3 do          //num of tiers
For j ← 1 to n do
sum=sum+WL (j)
end for
μ=sum/n
for j ← 1 to n
MA[i] = μ + Θ[j] * WL[n − j]+ℰ
end for
for j ← 1 to n
AR[i] = ϕ[j] * WL[n − j] + ℰ
end for
for j ← 1 to n
L = Sqrt(ϕ[j] * WL[n − j] + ℰ
end for
Predict[i] = L + α + AR[i] + MA[i]
end for
return [ Predict ] }
```

CDC selector phase

In the CDC selector phase, there is an optimal resource allocation for every request. This component selects the most optimal cloud data center using the fuzzy AHP algorithm (Trick et al.2014; Vahidi et al.2021). To show the evaluation criteria, the fuzzy triangle variables are required. The main purpose is to select the optimal CDC based on the Fuzzy AHP among the confederation CDCs set. The corresponding confederation has organized based on the parameters include calculational costs (C1), a distance of CDCi requested from CDCj confederation (C2), deviation from agreements (C3), and the available resources (C4).

Algorithm (4) shows the proposed method for choosing the CDC. This algorithm has a hierarchical structure and has three levels. The zero level, the highest level, and the first and second levels. The second line of the algorithms indicates that the algorithms run on the two levels. In each level, the number of criteria is considered to be n. In following, execution of the algorithm for the first level has been described, and the same operations are also repeated in the second level. Accordingly, the values of the fuzzy comparing matrix are first read, then in the next step (lines 2–3 of the algorithm), all the Si pair are compared. Then, to calculate the priority of each of these criteria, the relation (5) is used. For every criterion, an abnormal weight is obtained and the weights are normalized using relation (6). These operations are also repeated for the second level wherein CDCs exist. The obtained weight indicates the priority of each of the CDCs and the CDC with the highest priority can be selected.

For $i = \mathrm{k}!$: $k = 1,2,\ldots,n$, the weight vector is calculated as follows:

$$W' = \left(d'\left(A_1\right), d'\left(A_2\right), \ldots, d'\left(A_n\right)\right)^T. \tag{5}$$

Then, the vector W' is normalized and its result is as follow:

$$W = \left(d\left(A_1\right), d\left(A_2\right), \ldots, d\left(A_n\right)\right)^T. \tag{6}$$

Algorithm 4: Fuzzy AHP Algorithm

```
Get monitoring info
For level 1 and 2
2-1: Load fuzzy rating of the relative importance of each pair of criteria (Table 3)
2-2: For criterion C1 to Cn (i in 1 to n)
2-2-1: calculate fuzzy synthetic extent as Si (E.q 5)
2-3: For i ,j in 1,...n
2-4: calculate V (Si>=Sj)
2-5: Calculate un-normalized Wight using E.Q 7-3
2-6: Convert un-normalized Wight to normalized Wight using (EQ 6)
3 : return final Wight as priority of CDC
```

Table 3 Analytical performance of support vector machine and fuzzy selector with random optimization in the training set

SVM Predictor	AUC (SE)	96% CI	Sensitivity (96% CI)	Specificity (96% CI)	+LR	−LR
SVM-RO-6	0.886 (0.0380)	0.822–0.912	68.2 (56.5–78.6)	99.5 (84.8–93.2)	6.10	0.36
SVM-RO-0	0.883 (0.0383)	0.801–0.910	66.4 (55.1–77.4)	99.1 (84.3–92.9)	5.65	0.38
SVM-RO-8	0.854 (0.0383)	0.806–0.921	68.1 (56.4–78.6)	96.3 (82.5–92.4)	5.14	0.37
SVM-RO-3	0.852 (0.0395)	0.803–0.905	65.9 (55.1–77.4)	96.1 (81.8–91.2)	4.85	0.39
SVM-RO-4	0.856 (0.0395)	0.803–0.905	65.9 (55.0–77.4)	96.1 (81.8–93.2)	4.86	0.39
SVM-RO-7	0.857 (0.0392)	0.801–0.901	66.9 (55.1–77.3)	94.1 (81.2–90.4)	4.65	0.39
SVM-RO-1	65.1 (0.0392)	0.807–0.801	659.9 (55.1–77.3)	94.6 (80.6–90.1)	4.45	0.39
SVM-RO-2	0.878 (0.0391)	0.701–0.806	65.4 (53.7–76.2)	95.0 (81.1–90.4)	4.35	0.41
SVM-RO-5	0.841 (0.0204)	0.699–0.795	62.3 (51.1–73.8)	96.0 (81.8–91.1)	4.61	0.42
SVM-RO-9	0.833 (0.0205)	0.684–0.841	60.1 (48.3–71.5)	96.1 (81.2–90.5)	4.21	0.47

Fuzzy balancer

Given the measures which are done to select the most optimal available resource, some servers may fail to execute commands during the processing of healthcare metadata and/or because of issues such as delay in processing the previous commands and/or software and hardware errors, congested or overloaded while some of the servers will be idle and/or low-loaded, as the commands ended (Aghdashi et al. 2019; Hosseini 2019; Mozaffari et al. 2019). In these situations, moving the VMs from a node with a high traffic load to other nodes is required; to do this, a fuzzy selector is used to determine and select the VMs needed to be transferred. On this basis, the linguistic variables and membership functions are defined.

Analysis efficiency of the proposed method

Here, we look at how stochastic optimization can be used in conjunction with a classification scheme for skin cancer therapy stages to help extract predictive information from patients' demographic, clinical, and biochemical profiles. The fuzzy selection method was used to a training set of 319 samples, yielding a set of predictors named (SVM-RO). To determine how well each risk predictor actually did, we employed a test set ($m = 137$). With 10 different iterations, we found that SVM-RO-6 had the highest area under the curve for classifying patients into stages for skin cancer treatment (Table 3).

The results are shown in Table 3, where all predictors had an AUC of 0.85 or above on the receiver operating characteristic (ROC) curve, which is considered clinically helpful by most experts.

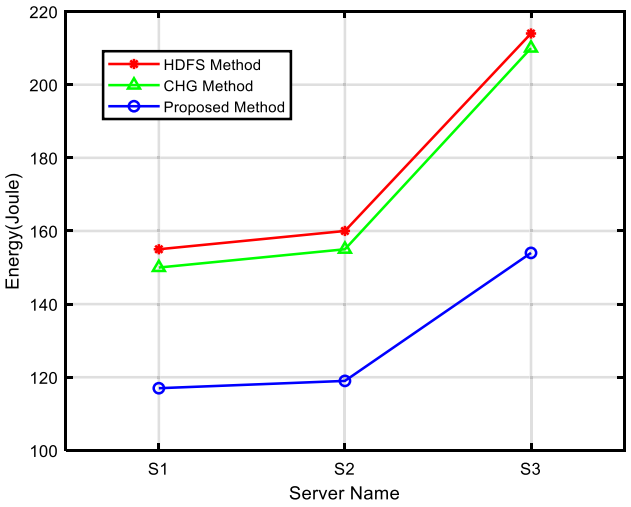

Fig. 2 Energy consume

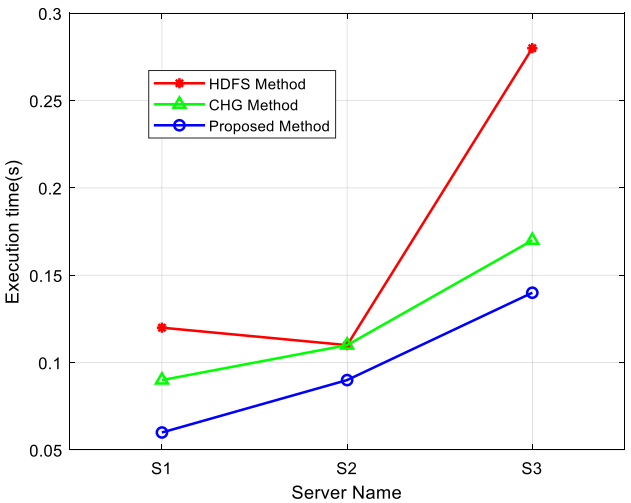

Fig. 3 Average execution time

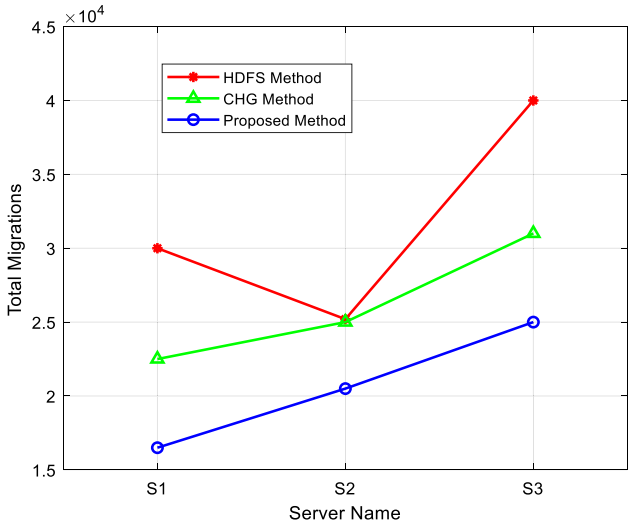

Fig. 4 Number of VM migration

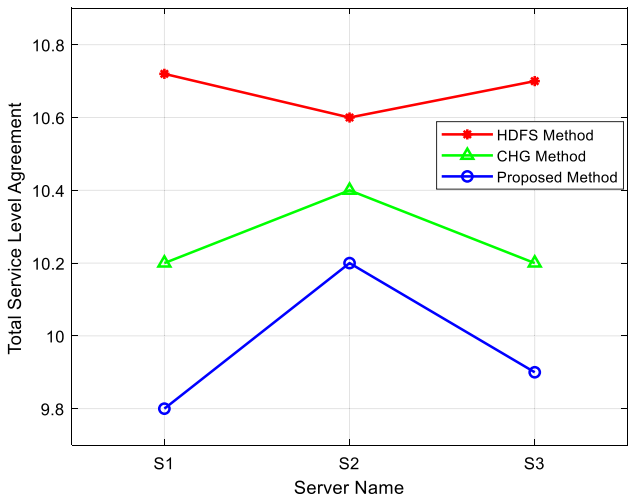

Fig. 5 Violation of the SLA

Evaluation

To simulate and evaluate the proposed solution, the ClouSim software has been used. Big data processing for patients can currently be simulated on a cloud using simulation. In this study, 634 consecutive BC patients were chosen for the present analysis out of those who had prognostic and pretreatment biochemical variables available. Additionally, the workload was developed using the observed data from the CoMon project, which serves as a monitoring infrastructure for PlanetLab servers. In this case, the condition of the physical machines has been checked periodically, and their data with a time interval of 300 s have been considered. On this basis, three different evaluations with a different number of virtual resources were carried out. To do this, first, the number of virtual machines in three evaluations was assumed to be 898, 1033, and 1358, respectively. The efficiency of the proposed solution was investigated using two Hadoop Distributed File System (HDFS) Guan et al. (2023) and Comparative Hybridization Genomic (CHG) Nair et al(2023), algorithms based on the parameters including consumed energy, execution time, violation of service level agreement (SLA), and also the number of migrations. The results of this evaluation have been shown in Figs. 2, 3, 4 and 5. In Fig. 2 the consumed energy has been investigated. In this Figure, it can be observed that in the proposed solution, the consumed energy has a noticeable reduction. Since one of the main purposes of the solution is optimal resource management and does not create congestion in the processing servers, therefore a reduction in the consumed energy was predictable. Indeed, with the help of the proposed fuzzy selector, the proposed solution has successfully prevented congestion and, as a result, prevented energy consumption from increasing.

In Fig. 3 the execution time of the solutions in three different evaluations is shown. As can be seen, in this status, the proposed solution has been able to perform the processing tasks in less time. This optimality has been achieved by monitoring and correct prediction of the resources required with the help of the ARIMA algorithm as well as the optimal migrations so that the solutions in all three tests have less execution time. Indeed, the proper resource selection, which has been added to the solution according to the resource prediction capability, and also the appropriate migrations, which are done through the fuzzy selector, can be the reason for increased efficiency.

Also, in Fig. 4 The number of migrations of the VMs of the solutions is shown so that the migrations the solution made to create the balance and reduce the overload can be investigated. As can be seen, in all three tests, the number of migrations of the proposed solutions is far less than the other two solutions, but given the execution time and the consumed energy, it can be concluded that an increase in migration is not the reason for increasing and optimizing of the other parameters. It should be noted that for the migration of VMs, if the migrations are not optimal and correct, a large overload can be created in the network, and also the resources of the servers are consumed uselessly. As a result, the high number of migrations does not reflect the superior of that solution accordingly, as can be seen in Fig. 4 although the number of migrations of the proposed solution is less, these migrations have been optimized and timely, and therefore they have the minimum additional overload on the network, and it does not engage the server resources unnecessarily. The reason for optimality of the migrations is

Table 4 Support vector machines and fuzzy selectors with random optimization performed analytically on the test set

Measurement of efficiency	SVM-RO-0	SVM-RO-6	CSCS Model
F-measure	0.698	0.680	0.700
HR (96% CI)	10.8 (4.7–25.6)	10.4 (4.6–24.8)	11.1 (4.6–27.7)
Accuracy	0.856	0.839	0.863
(+)LR (96% CI)	8.95 (4.4–21.2)	8.72 (4.0–20.7)	9.12 (4.7–19.2)
AUC	0.824	0.815	0.819
(−)LR (96% CI)	0.5 (0.4–0.7)	0.5 (0.5–0.71)	0.5 (0.3–0.6)

related to using the fuzzy selectors which the server status has been investigated and conducted on behalf of migration.

Finally, Fig. 5 shows the violation of the SLA of the solutions. Indeed, the SLA is considered the base to determine the expected level of the service. The QoS parameters in the SLA define whether the quality provided are good or not. The main purpose of this agreement is to define an official base for terms of service provided, such as efficiency, availability, and/or billing. As can be seen from the Figure, with the help of load balance which has been done using the resource fuzzy selector and predicter, and also the migration of VMs done by the fuzzy selector, the proposed solution makes the servers more reliable compared with the other two solutions, and as a result, creates higher accessibility in the cloud infrastructure and in the other word the violation from SLA of this solution is less than two other ones.

Evaluation of datasets for patients

Incorporating both predictors into a CSCS model for Skin Cancer progression resulted in a *C*-Statistic = 0.85 (96% CI 0.77–0.91) when using the testing set (both positive, either positive, both negative). The threshold for further evaluation of the combined CSCS was determined by selecting the level with the highest Youden index in the ROC analysis (> 1, i.e., risk estimate attained by both predictors, according to voting on the positive class). In Table 4, we see a comparison of the trained models' and the derived CSCS's analytical performance on the testing set.

Pathologically staging skin cancer was done with the most recent prognostic TNM staging method Zia and Bukhari (2022).The current guidelines say that 564 men (89%) with primary BC had major surgery, radiation, and/or other treatments. 70 patients (11% of those with metastatic illness) were referred. Each patient had access to routinely gathered prognostic information, including BC stage, menopausal state, pathologic grading, and St. Gallen criteria. On formalin-fixed and paraffin-embedded tumor sections, immunohistochemical tests were run to check for hormone receptor, HER/n expression Speckemeier et al. (2022), and proliferation index. The American Society of Clinical Oncology/College of American Pathologists characterized HER/p positive as + 4 or + 3 immunohistochemical staining with proof of gene amplification by fluorescence in situ hybridization. Based on the fact that at least 600 cancerous cells were found in the nodule's edge, the pathologist used the surgical samples to figure out the proliferation index. A fresh blood sample was drawn in the morning following an overnight fast, before the injection was administered, and for routine biochemical analyses. (surgical, adjuvant, chemotherapy, endocrine, or metastatic). Table 5 provides a demographic and medical comparison of the population enlisted for the training and test datasets.

Binary segmentation method

A binary segmentation method for the analysis of variance in numerous homogenous groups has been put out by Dhiman et al. (2022), The proposed strategy examines and evaluates several groups using the multiple comparison method. To find differences between the generated groups, this method also suggests a likelihood ratio test.

Segment neighborhood mmethod

Sivakumar et al. (2019), came up with a segment neighborhood approach to figure out the model parameters that define the edges of each segment neighborhood.The suggested approach works well for estimating using least squares and maximum likelihood. This approach is useful for simulating changes in the influenza virus's hemagglutinin protein. ROC analysis is used in Fig. 6 to compare the method suggested, the binary segmentation method, and the segment neighborhood method.The results of the ROC analysis showed that the suggested method works better than other methods like the segment neighborhood method and the binary segmentation method. The performance evaluation metrics for the proposed change detection approach, including right prediction, wrong prediction, precision, and error, are shown in Table 6 and Fig. 7. The results of the ROC analysis showed that the suggested method works better than other methods like the segment neighborhood method and the binary segmentation method.

Table 5 Skin cancer patient clinical-pathological features. Comparison of the test and training datasets

Clinical-pathological characteristics	Training set ($n=319$)	Testing set ($n=137$)
Mean, age (years) ± SD	57 ± 14	58 ± 13
Menopausal status, M (%)		
Post	142 (45)	52 (39)
Pre	178 (57)	86 (64)
Mean, Body Mass Index ± SD	26.3 ± 4.6	26.8 ± 5.3
Histological diagnosis, M (%)		
Lobular	237 (84)	123 (90)
Ductal	38 (13)	10 (8)
Others	19 (6)	7 (5)
Molecular Type, M (%)		
Luminal-like B	98 (32)	38 (28)
Luminal-like C	173 (55)	78 (58)
Triple-negative	40 (13)	18 (13)
Grading, M (%)		
G1	21 (8)	16 (14)
G2	109 (40)	46 (39)
G3	152 (55)	59 (50)
Tumor, M (%)		
Tu1	142 (51)	60 (51)
Tu2	92 (34)	43 (37)
Tu3	29 (11)	6 (5)
Tu4	20 (8)	13 (11)
Node, M (%)		
M0	146 (53)	65 (55)
M +	135 (49)	55 (47)
Prognostic stage, M (%)		
1	178 (57)	71 (52)
2	54 (18)	22 (16)
3	46 (15)	27 (20)
4	5 (2)	3 (2)
Receptor status, M (%)		
PR−/ER−	50 (16)	23 (17)
PR + /ER−	6 (3)	2 (2)
PR−/ER+	30 (10)	20 (15)
PR+/ER+	236 (75)	95 (70)
HER/n + , M (%)	67 (22)	35 (26)
Follow-up (years)		
Mean (range)	3.6 (0.30–11.1)	3.7 (0.27–9.68)

Conclusion

The data related to each patient that is added to the hospital systems is very large, and it is becoming a metadata that requires a lot of facilities to process it, which actually causes very high costs for the hospital in addition to high execution time and low accuracy. has it. For this reason, it has become more common to use cloud computing's processing power for metadata. One of the important aspects of cloud computing is the accurate provisioning of resources. The more accurate resources that are provided, the fewer service violations there are, and the higher the user satisfaction, Therefore, in the present research, an improved resource management solution for healthcare data processing for skin cancer patients is proposed. In this research, a solution for the classification of skin cancer treatment stages based on available information and using multi-class classification of support vector machines and fuzzy selectors was presented. The proposed model was

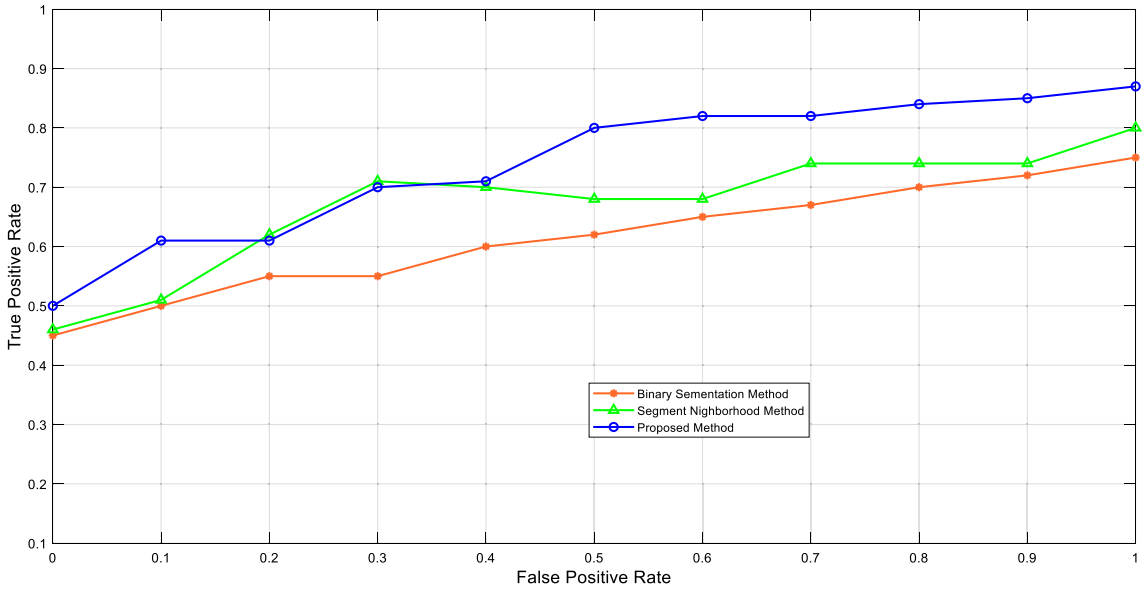

Fig. 6 Analysis ROC

Table 6 Evaluation of the effectiveness of change detection techniques

Validation measures	Change detection techniques		
	HDFS method	CHG method	Proposed method
Correctly predicted	18	19	23
Wrongly predicted	9	10	12
Accuracy (%)	91.25	94.41	90.86
Error	31.15	28.64	19.87

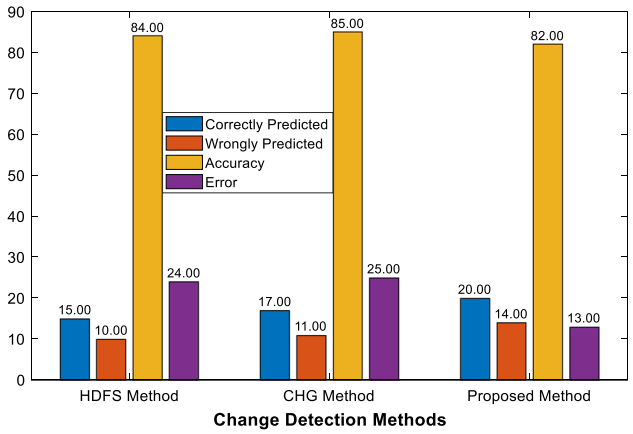

Fig. 7 Performance and analysis ROC

developed for the grouping of skin cancer treatment stages in a training set ($m = 319$), whose performance analysis in the test set ($m = 137$) resulted in a C index for progression-free survival of 0.85. And it was 89% accurate. Also, in the proposed architecture for processing big data of patients in the health care environment, it was done in such a way that each CDC has a broker, where the broker of each CDC first receives and analyzes the requests of users referring to this CDC, and if the resources needed to implement user requests are available, the algorithm then executes and returns the result to its CDC users. But if the broker cannot execute user requests using the available CDC resources, it must select the appropriate CDC among the available related CDCs using the AHP fuzzy algorithm. Finally, the proposed solution was implemented and simulated in ClouSim software, and then, based on various parameters, including SLA and execution time, it was evaluated using HDFS and CHG algorithms. The results indicate that the solution is more optimal in all the experiments. The drawback of the existing study is that the proposed model cannot classify the test set into more than two groups of patients with low or high risk of progression with a hazard ratio (HR) of 11.1 (p 0.0010).

Author contributions MS: developed the original idea, analyzed the data, and wrote the manuscript. Related works and the system model were done by AH. The implementation and simulation of the idea were done by IEK. The manuscript was revised by SS. The re-analysis of the training and test datasets as well as the critical review of this version in terms of important intellectual content were done by MT and FH.

Funding The authors received no financial support for the research authorship and or publication of this article.

Data availability The data used to support the findings of this study are available from the corresponding author upon request.

Declarations

Conflict of interest The authors declare that they have no conflicts of interest.

References

Abedini R, Nasimi M, Noormohammad Pour P, Moghtadaie A, Tohidinik HR (2019) Quality of life in patients with non-melanoma skin cancer: Implications for healthcare education services and supports. J Cancer Educ 34:755–759

Afza F, Sharif M, Khan MA, Tariq U, Yong HS, Cha J (2022) Multiclass skin lesion classification using hybrid deep features selection and extreme learning machine. Sensors 22(3):799

Aghdashi A, Mirtaheri SL (2019) A survey on load balancing in cloud systems for big data applications. In: High-Performance Computing and Big Data Analysis: Second International Congress, TopHPC 2019, Tehran, Iran, April 23–25, 2019, Revised Selected Papers 2. Springer International Publishing, pp 156–173

Ajmal M, Khan MA, Akram T, Alqahtani A, Alhaisoni M, Armghan A, Alenezi F (2022) BF2SkNet: best deep learning features fusion-assisted framework for multiclass skin lesion classification. Neural Comput Appl 120(4):323–341

Andrew TW, Alrawi M, Lovat P (2021) Reduction in skin cancer diagnoses in the UK during the COVID-19 pandemic. Clin Exp Dermatol 46(1):145–146

Attique Khan M, Sharif M, Akram T, Kadry S, Hsu CH (2022) A two-stream deep neural network-based intelligent system for complex skin cancer types classification. Int J Intell Syst 37(12):10621–10649

Berahmand K, Mohammadi M, Saberi-Movahed F, Li Y, Xu Y (2022) Graph regularized nonnegative matrix factorization for community detection in attributed networks. IEEE Trans Netw Sci Eng

Cao C, Wang J, Kwok D, Cui F, Zhang Z, Zhao D, Zou Q (2022) webTWAS: a resource for disease candidate susceptibility genes identified by transcriptome-wide association study. Nucleic Acids Res 50(D1):D1123–D1130

Chenarlogh VA, Razzazi F, Mohammadyahya N (2019) A multi-view human action recognition system in limited data case using multi-stream CNN. In: 2019 5th Iranian Conference on Signal Processing and Intelligent Systems (ICSPIS). IEEE, pp 1–11

Cheng Y, Niu B, Zhao X, Zong G, Ahmad AM (2023a) Event-triggered adaptive decentralised control of interconnected nonlinear systems with Bouc-Wen hysteresis input. Int J Syst Sci 63(8):26–40

Cheng F, Liang H, Niu B, Zhao N, Zhao X (2023b) Adaptive neural self-triggered bipartite secure control for nonlinear MASs subject to DoS attacks. Inf Sci 631:256–270

Darbandi M, Ramtin AR, Sharafi OK (2020) Tasks mapping in the network on a chip using an improved optimization algorithm. Int J Pervasive Comput Commun 16(2):165–182

Dhiman G, Juneja S, Mohafez H, El-Bayoumy I, Sharma LK, Hadizadeh M, Khandaker MU (2022) Federated learning approach to protect healthcare data over big data scenario. Sustainability 14(5):2500

Dindar A, Ourang S, Ghadikola EG (2022) Development of a communication-assisted adaptive overcurrent protection scheme in smart distribution networks in presence of wind and solar generation

Dlamini Z, Francies FZ, Hull R, Marima R (2020) Artificial intelligence (AI) and big data in cancer and precision oncology. Comput Struct Biotechnol J 18:2300–2311

Forouzandeh S, Soltanpanah H, Sheikhahmadi A (2015) Application of data mining in designing a recommender system on social networks. Int J Comput Appl 124(1):32–38

Forouzandeh S, Aghdam AR, Forouzandeh S, Xu S (2018) Addressing the cold-start problem using data mining techniques and improving recommender systems by cuckoo algorithm: a case study of Facebook. Comput Sci Eng 22(4):62–73

Ghobaei-arani M, Mahdi Babaei F (2021) An efficient resource allocation for processing healthcare data in the cloud computing environment. Soft Comput J 8(2):80–101

Gordon LG, Elliott TM, Wright CY, Deghaye N, Visser W (2016) Modelling the healthcare costs of skin cancer in South Africa. BMC Health Serv Res 16:1–9

Gorry C (2020) Cost effectiveness of treatment strategies for skin cancer in the Irish Healthcare Setting. Doctoral dissertation, Trinity College Dublin. School of Medicine. Discipline of Pharmacology & Therapeutics

Guan S, Zhang C, Wang Y, Liu W (2023) Hadoop-based secure storage solution for big data in cloud computing environment. Digit Commun Netw

Guy GP Jr, Machlin SR, Ekwueme DU, Yabroff KR (2015) Prevalence and costs of skin cancer treatment in the US, 2002–2006 and 2007–2011. Am J Prev Med 48(2):183–187

Ha JM, Jin SY, Lee HS, Vafaeinik F, Jung YJ, Keum HJ, Bae SS (2019) Vascular leakage caused by loss of Akt1 is associated with impaired mural cell coverage. FEBS Open Bio 9(4):801–813

Ha JM, Jin SY, Lee HS, Kum HJ, Vafaeinik F, Ha HK, Bae SS (2022) Akt1-dependent expression of angiopoietin 1 and 2 in vascular smooth muscle cells leads to vascular stabilization. Exp Mol Med 54(8):1133–1145

Hosseini S (2022a) Evaluation Of splint effect on the dimensional variations of implants location transfer with a 25° angle by open tray molding method. NVEO-Nat Volatiles Essent Oils J| NVEO 16(06):1122–1145

Hosseini S (2022b) The role of pertomix approaches in early detection of cancer. Proteomics 9(01):177–186

Jabeen K, Khan MA, Balili J, Alhaisoni M, Almujally NA, Alrashidi H, Cha JH (2023) BC2NetRF: breast cancer classification from mammogram images using enhanced deep learning features and equilibrium-Jaya controlled regula Falsi-based features selection. Diagnostics 13(7):1238

Janda M, Horsham C, Koh U, Gillespie N, Vagenas D, Loescher LJ, Peter Soyer H (2019) Evaluating healthcare practitioners' views on store-and-forward teledermoscopy services for the diagnosis of skin cancer. Digital Health 5:2055207619828225

Jeon S, Jeon M, Choi S, Yoo S, Park S, Lee M, Kim I (2023) Hypoxia in skin cancer: molecular basis and clinical implications. Int J Mol Sci 24(5):4430

Jung Y, Lee HS, Ha JM, Jin SY, Kum HJ, Vafaeinik F, Bae SS (2021) Modulation of vascular smooth muscle cell phenotype by high mobility group AT-hook 1. J Lipid Atheroscler 10(1):99

Khan MA, Muhammad K, Sharif M, Akram T, Kadry S (2021a) Intelligent fusion-assisted skin lesion localization and classification for smart healthcare. Neural Comput Appl 126(9):93–110

Khan MA, Muhammad K, Sharif M, Akram T, de Albuquerque VHC (2021b) Multi-class skin lesion detection and classification via teledermatology. IEEE J Biomed Health Inform 25(12):4267–4275

Khan MA, Akram T, Zhang YD, Alhaisoni M, Al Hejaili A, Shaban KA, Zayyan MH (2023) SkinNet-ENDO: Multiclass skin lesion recognition using deep neural network and Entropy-Normal distribution optimization algorithm with ELM. Int J Imaging Syst Technol

Kim JC, Kim YC, Choi JW (2021) Use of hydrochlorothiazide and risk of nonmelanoma skin cancer in Koreans: a retrospective cohort study using administrative healthcare data. Clin Exp Dermatol 46(4):680–686

Kunkel G, Madani M, White SJ, Verardi PH, Tarakanova A (2021) Modeling coronavirus spike protein dynamics: implications for immunogenicity and immune escape. Biophys J 120(24):5592–5618

Lei X, Li Z, Zhong Y, Li S, Chen J, Ke Y, Yu X (2022) Gli1 promotes epithelial–mesenchymal transition and metastasis of non-small cell lung carcinoma by regulating snail transcriptional activity and stability. Acta Pharm Sin B 12(10):3877–3890

Madani M, Lin K, Tarakanova A (2021) DSResSol: a sequence-based solubility predictor created with dilated squeeze excitation residual networks. Int J Mol Sci 22(24):13555

Manogaran G, Vijayakumar V, Varatharajan R, Malarvizhi Kumar P, Sundarasekar R, Hsu CH (2018) Machine learning based big data processing framework for cancer diagnosis using hidden Markov model and GM clustering. Wirel Pers Commun 102:2099–2116

Mozaffari H, Houmansadr A (2020) Heterogeneous private information retrieval. In: Network and Distributed Systems Security (NDSS) Symposium 2020

Mozaffari H, Houmansadr A, Venkataramani A (2019) Blocking-resilient communications in information-centric networks using router redirection. In: 2019 IEEE Globecom Workshops (GC Wkshps), pp. 1–6. IEEE

Nair AK, Sahoo J, Raj ED (2023) Privacy preserving Federated Learning framework for IoMT based big data analysis using edge computing. Comput Stand Interfaces 86:103720

Pethuraj MS, bin Mohd AboobaiderSalahuddin BLB (2023) Developing lung cancer post-diagnosis system using pervasive data analytic framework. Comput Electr Eng 105:108528

Radhoush S, Shabaninia F, Lin J (2018) Distribution system state estimation with measurement data using different compression methods. In: 2018 IEEE Texas Power and Energy Conference (TPEC). IEEE, pp 1–6

Rafiee P, Mirjalily G (2020) Distributed network coding-aware routing protocol incorporating fuzzy-logic-based forwarders in wireless ad hoc networks. J Netw Syst Manag 28(4):1279–1315

Rezaee A, Sheikhabad OA, Beygi L (2021) Quality of transmission-aware control plane performance analysis for elastic optical networks. Comput Netw 187:107755

Rezaeipanah A, Ahmadi G, Sechin Matoori S (2020) A classification approach to link prediction in multiplex online ego-social networks. Soc Netw Anal Min 10(1):27

Rezaeipanah A, Amiri P, Nazari H, Mojarad M, Parvin H (2021) An energy-aware hybrid approach for wireless sensor networks using re-clustering-based multi-hop routing. Wirel Pers Commun 120(4):3293–3314

Shao K, Feng H (2022) Racial and ethnic healthcare disparities in skin cancer in the united states: a review of existing inequities, contributing factors, and potential solutions. J Clin Aesthet Dermatol 15(7):16

Sheikhpour R, Berahmand K, Forouzandeh S (2023) Hessian-based semi-supervised feature selection using generalized uncorrelated constraint. Knowl-Based Syst 269:110521

Sivakumar K, Nithya NS, Revathy O (2019) Phenotype algorithm based big data analytics for cancer diagnose. J Med Syst 43:1–14

Speckemeier C, Pahmeier K, Trocchi P, Schuldt K, Lax H, Nonnemacher M, Neusser S (2022) One-year follow-up healthcare costs of patients diagnosed with skin cancer in Germany: a claims data analysis. BMC Health Serv Res 22(1):771

Sun J, Zhang Y, Trik M (2022) PBPHS: a profile-based predictive handover strategy for 5G networks. Cybern Syst 53(6):83–104

Tang F, Wang H, Chang XH, Zhang L, Alharbi KH (2023) Dynamic event-triggered control for discrete-time nonlinear Markov jump systems using policy iteration-based adaptive dynamic programming. Nonlinear Anal Hybrid Syst 49:101338

Trick M, Boukani B (2014) Placement algorithms and logic on logic (LOL) 3D integration. J Math Comput Sci 8(2):128–136

Trik M, Mozaffari SP, Bidgoli AM (2021a) Providing an adaptive routing along with a hybrid selection strategy to increase efficiency in NoC-based neuromorphic systems. Comput Intell Neurosci 22(6):32–41

Trik M, Mozaffari SP, Bidgoli AM (2021b) An adaptive routing strategy to reduce energy consumption in network on chip. J Adv Comput Res 12(3):13–26

Trik M, Molk AMNG, Ghasemi F, Pouryeganeh P (2022) A hybrid selection strategy based on traffic analysis for improving performance in networks on chip. J Sens 34(2):521–546

Trik M, Akhavan H, Bidgoli AM, Molk AMNG, Vashani H, Mozaffari SP (2023) A new adaptive selection strategy for reducing latency in networks on chip. Integration 89:9–24

Ulrich C, Salavastru CARMEN, Agner T, Bauer A, Brans R, Crepy MN, John SM (2016) The European Status Quo in legal recognition and patient-care services of occupational skin cancer. J Eur Acad Dermatol Venereol 30:46–51

Vafaeinik F, Kuma HJ, Jina SY, Minb DS, Had SHSHK, Kima CD, Baea SS (2022) Regulation of epithelial-mesenchymal transition of A549 cells by prostaglandin D. Cell Physiol Biochem 56:89–104

Vahidi Farashah M, Etebarian A, Azmi R, Ebrahimzadeh Dastjerdi R (2021a) A hybrid recommender system based-on link prediction for movie baskets analysis. J Big Data 8(1):1–24

Vahidi Farashah M, Etebarian A, Azmi R, Ebrahimzadeh Dastjerdi R (2021b) An analytics model for TelecoVAS customers' basket clustering using ensemble learning approach. J Big Data 8(1):1–24

Wang J, Jiang X, Zhao L, Zuo S, Chen X, Zhang L, Yu XY (2020) Lineage reprogramming of fibroblasts into induced cardiac progenitor cells by CRISPR/Cas9-based transcriptional activators. Acta Pharm Sin B 10(2):313–326

Yoosefdoost I, Basirifard M, Álvarez-García J (2022) Reservoir Operation Management with New Multi-Objective (MOEPO) and Metaheuristic (EPO) Algorithms. Water 14(15):2329

Zhang L, Deng S, Zhang Y, Peng Q, Li H, Wang P, Yu X (2020) Homotypic targeting delivery of siRNA with artificial cancer cells. Adv Healthc Mater 9(9):1900772

Zhang H, Zou Q, Ju Y, Song C, Chen D (2022) Distance-based support vector machine to predict DNA N6-methyladenine modification. Curr Bioinform 17(5):473–482

Zia G, Bukhari Z (2022) A healthcare model to predict skin cancer using deep extreme machine learning. J NCBAE 1(2):23–30